Dyes and Pigments 200 (2022) 110149

Contents lists available at ScienceDirect

Dyes and Pigments

journal homepage: www.elsevier.com/locate/dyepig

Benzotriazole-based multidonor-acceptor systems as attractive two-photon absorption dye platforms

Carlos Benitez-Martin [a,b,1], Beatriz Donoso [c,1], Iván Torres-Moya [c], Jesús Herrera [c], Ángel Díaz-Ortiz [c], Francisco Najera [a,b,**], Pilar Prieto [c,***], Ezequiel Perez-Inestrosa [a,b,*]

[a] Universidad de Málaga-IBIMA, Departamento de Química Orgánica, 29071, Málaga, Spain
[b] Centro Andaluz de Nanomedicina y Biotecnología (BIONAND), Parque Tecnológico de Andalucía, 29590, Málaga, Spain
[c] Department of Organic, Inorganic Chemistry and Biochemistry, Faculty of Chemical and Technologies Sciences-IRICA, Universidad de Castilla-La Mancha, 13071, Ciudad Real, Spain

ARTICLE INFO

Keywords:
Two-photon absorption
Fluorescence
DFT calculations
Benzotriazole dyes

ABSTRACT

Pyrazine-decorated benzotriazole cores allow the orthogonal combination of two dipolar systems within a single molecule. A series of this type of derivatives was synthesized and their photophysical features were studied. The properties of these compounds showed remarkable differences in function depending on the substitution in the pyrazine ring of the benzotriazole core. Furthermore, the two-photon absorption property (2PA) was studied to determine the structure-properties relationship for the reported compounds. The best dye achieved a cross-section of 1532 GM, which was higher than values previously obtained for similar D-π-A-π-D benzotriazole derivatives. TD-DFT calculations, which supported the experimental observations, indicating the interaction between the two dipolar systems was responsible for enhancing the 2 PA properties and favoring bathochromic shifts.

1. Introduction

Owing to the three-dimensional control of the excitation process, the use of two-photon absorption (2PA) has featured in multiple applications, including bioimaging [1–3], microfabrication [4–7], optical storage [8–12], and others [13,14]. Accordingly, major research efforts have been focused on the development of specifically designed organic two-photon (2P)-chromophores. These type of dyes, resulting from the dipolar approach of the 2PA process [15], consists essentially of *push--pull* architectures in which electron-donor (D) and electron-acceptor (A) groups are usually connected *via* a π-conjugated system. Hence, according to this model, an association between intramolecular charge transfer [16] and 2PA properties can be inferred [17–19], although this is not the only key element that provides the 2P-chromophore with useful features. Other elements, such as the enlargement of the conjugation, the increment in the coplanarity in the D-π-A system [20] and even the formation of rigid structures between the donor and acceptor together in a single system have to be taken into account [21]. The symmetry of the structure is also a determinant of the 2PA cross-section (σ_{2PA}), and structural schemes, such as quadrupolar (D-π-D, A-π-A, D-A-D, A-D-A, D-π-A-π-D, A-π-D-π-A, etc.), octopolar (dendrimer-like combinations of dipolar motifs) and multi-branched molecules, have been demonstrated to confer excellent 2PA ability. By following these guidelines, a large number of dyes with improved 2PA features have been described, and these studies have consequently guided the design of new 2P-dyes [22,23].

Among this wide variety of structural models devised for 2P-chromophores, benzoazole derivatives have been well studied in recent years, especially those based on 1,2,5-benzothiadiazoles (BTDs) [24–28]. These compounds stand out from others mainly owing to their synthetic versatility and readily tunable photophysical properties, which permit diverse uses, such as 2P-bioimaging [29,30], optical limiting [31,32], and others [33–35]. Although less well explored, 2*H*-benzo[*d*] [1–3] triazole (BTz) derivatives are an interesting alternative to BTD, offering comparable synthetic and optical flexibility [36,37]. In addition, we have recently described D-π-A-π-D alkynyl-BTz derivatives with large

* Corresponding author. Universidad de Málaga-IBIMA, Departamento de Química Orgánica, 29071, Málaga, Spain.
** Corresponding author. Universidad de Málaga-IBIMA, Departamento de Química Orgánica, 29071, Málaga, Spain.
*** Corresponding author. Universidad de Castilla-La Mancha-IRICA, Departamento de Química Inorgánica, Orgánica y Bioquímica, 3071, Ciudad Real, Spain.
E-mail addresses: najera@uma.es (F. Najera), Mariapilar.prieto@uclm.es (P. Prieto), inestrosa@uma.es (E. Perez-Inestrosa).
[1] C.B.-M. and B.D. contributed equally to this article.

https://doi.org/10.1016/j.dyepig.2022.110149
Received 27 December 2021; Received in revised form 26 January 2022; Accepted 28 January 2022
Available online 3 February 2022

Stokes shifts and good fluorescence quantum yields (φ_F) together with σ_{2PA} values of up to 1510 GM [28].

Encouraged by these precedents, we have reported herein a new family of alkynyl-BTz dyes combining two dipolar chromophores in the same structure, *i.e.*, a unique BTz acceptor core electronically encounters two different donor groups through the two axes of the molecule (Fig. 1). Thereby, in these dyes, we can distinguish a D-π-A-π-D pattern in the horizontal axis, and a D-A system in the vertical axis. To allow this orthogonal combination, as well as the incorporation of new donor groups to the structure, the BTz unit was decorated at the top with a pyrazine ring, resulting in a [1–3]triazolo[4,5-*g*]quinoxaline core (hereinafter referred as TzQ). The integration of this TzQ moiety implies the increased acceptor character of the central core, and consequently, enhanced π-conjugation along the scaffold.

Although the incorporation of a pyrazine ring to BTD derivatives has been reported [38–41], its effect on the 2PA properties has not yet been described. Therefore, this work aims to explore the structure-property relationships that are derived from this relatively unexplored concept for building 2P-chromophores. That is, we intend to evaluate the possible mutual influence between the diverse dipolar motifs integrated in the same structure, and its outcomes on the overall optical properties. Theoretical calculations are performed to achieve better understanding about the behavior of these systems.

2. Results and discussion

2.1. Synthesis

Derivatives **6** were prepared starting from our previously described dibromo benzotriazole derivative **1** (Scheme 1) [42]. To build the pyrazine moiety, nitration of this compound with HNO_3/CF_3SO_3H was performed to afford derivative **2**. The nitro compound was reduced to the diamine intermediate **3** in excellent yield (94%) by the use of Fe in acetic acid at room temperature [43]. The condensation of **3** with 1, 2-diketones **4a**–**e** formed the pyrazine moiety, giving the tricyclic compounds **5a**–**e** in acceptable to good yields (62%–88%) (Scheme 1) [44].

Compounds **4b** and **c** are available from commercial suppliers, and diketones **4a**, **d**, and **e** are known substrates and were prepared in accordance with following procedure: from freshly distilled oxalyl chloride: a Friedel-Crafts reaction with commercially available dodecylbenzene afforded diketone **4a** in 50% yield [45], whereas an aromatic substitution with the readily available 3-bromothiophene gave **4d** in 16% yield [46]. Finally, an oxidative ring closing of **4d** using iron tribromide in dichloromethane allowed us to obtain **4e** in 66% yield [46].

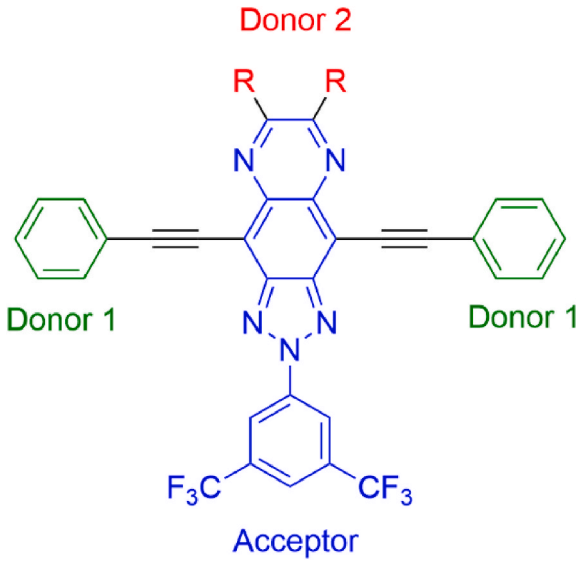

Fig. 1. General structure of the multidonor-acceptor systems based on TzQ presented in this work. A range of electron-donor groups (highlighted in green and red) can be linked to a same electron-acceptor core (blue), leading to two electronically connected orthogonal dipolar chromophores.

In the last step, the microwave-assisted Stille C–C cross-coupling reaction [47], which is well-established by our research group, was performed between **5a**–**e** and tributyl(phenylethynyl)stannane in the presence of $Pd(Ph_3)_2Cl_2$/LiCl and allowed us to prepare the alkynyl [1–3]triazolo[4,5-*g*]quinoxaline derivatives **6a**–**e** within 20 min in acceptable to good yields (51%–92%) (Scheme 1). These compounds were purified by means of column chromatography on silica gel employing hexane/ethyl acetate as the eluent. The known derivatives were characterized on the basis of their reported data. Satisfactory analytical MS and NMR spectroscopy data for the new compounds, **2**, **3**, **5a**–**e**, and **6a**–**e**, were obtained. (Experimental data and NMR spectra are incorporated in the Supporting Information).

2.2. Photophysical properties under one-photon excitation conditions

The photophysical properties of compounds in series **6** were examined in chloroform solution. The corresponding data are summarized in Table 1, while the representative absorption bands and the emission spectra of these compounds are presented in Fig. 2.

These dyes are characterized by their intricate absorption spectra, which are composed of multiple contributions from the two integrated chromophores; the complete absorption spectra are in Fig. S1. With regard to the spectral position, the longest-wavelength (LW) absorption bands are centered between 529 and 633 nm according to effective π-conjugation. Dyes **6a**, **c**, and **d**, which have vertical donor groups that can rotate, have peaks at higher-energy wavelengths. Among them, the weaker electron-donor character of phenyl *vs.* thiophene results in the largest blue-shifted absorption for **6a**. Furthermore, compound **6c** exhibits a slight bathochromic shift compared with **6d**, which is in accordance with the character of π-excessive heterocycles and the effect of the connecting position of thiophene. In contrast, rotation is prevented in **6b** and **6e** by covalently linking the donor groups on the vertical axis. Consequently, these dyes achieve improved electronic movement, and their absorptions occur in the red spectral region. Derivative **6e**, bearing the best electron-donor group, has a LW absorption maximum at 633 nm.

With regard to the emission spectra, these analogs display bands with maxima between 595 and 670 nm. It is worth noting that in terms of spectral position, the observations made above for the absorption bands also apply for the emission ones. Thus, the most red-shifted emissions were observed for **6b** and **6e** (Table 1). Moreover, the fluorescence quantum yields of these derivatives were moderate to good (*ca.* 0.2–0.7), and were complemented by fluorescence lifetimes that range from approximately 6 to 11 ns (Table 1) Additionally, the rates of radiative and non-radiative rates were calculated for each compound (Table S1), these explaining the trends drawn in fluorescence quantum yields (see Supporting Information, Section 5.1).

From these data, it appears that the influence of the vertical dipolar system on the optical properties of **6a**, **c**, and **d** is mild, with no substantial differences observed between their features. In contrast, the remarkable bathochromic shifts noted in **6b** and **6e** could be partially explained by the electronic communication between the chromophores at the different axes (see Table 1). To gain insights into this behavior, DFT and TD-DFT calculations were performed. The geometries were first optimized at the PCM($CHCl_3$)/CAM-B3LYP/6-31G(d) level, and absorption and emission energies were then calculated at the PCM ($CHCl_3$)/CAM-B3LYP/6-311+G(2d,p)//PCM($CHCl_3$)/CAM-B3LYP/6-31G(d) level. The comparison between experimental and theoretical absorption and emission energies is summarized in Table 2.

This methodology is extremely accurate for the prediction of

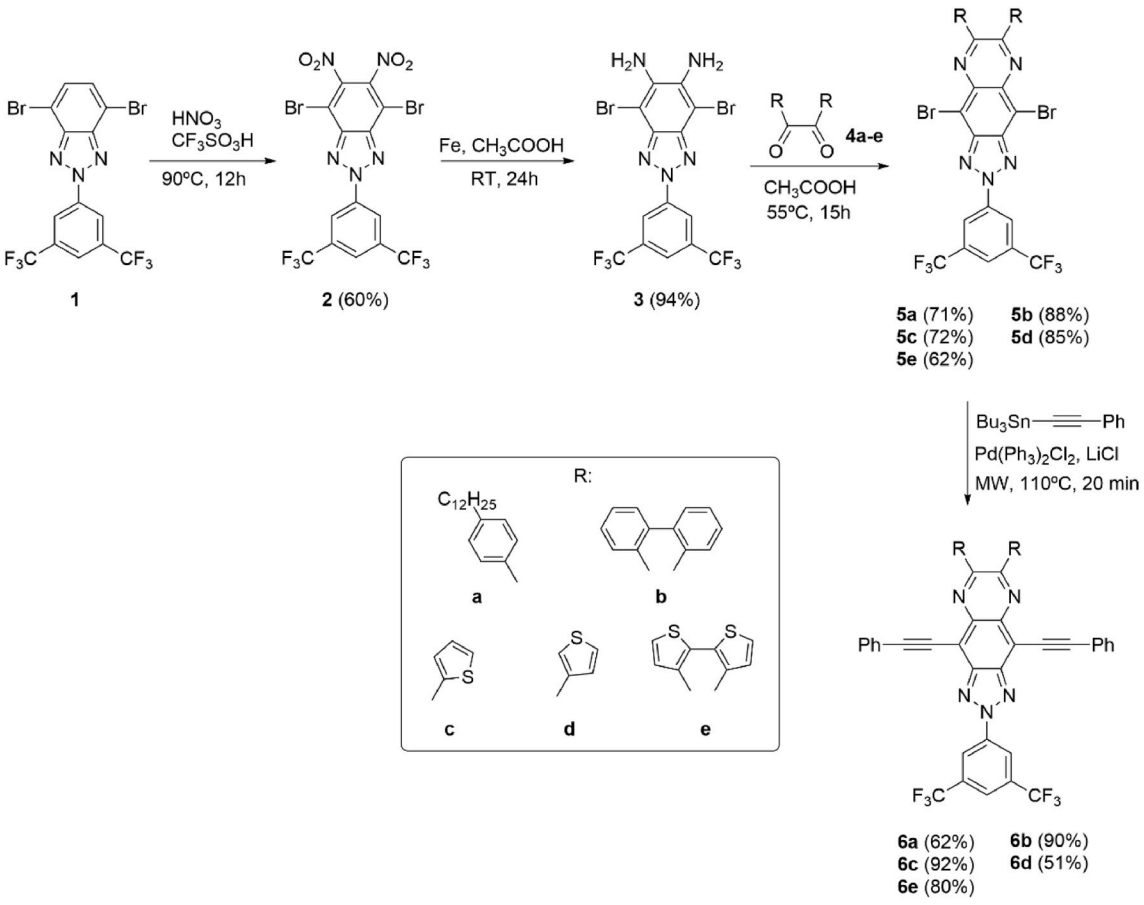

Scheme 1. Synthetic route for the preparation of compounds **6a**–**e** from BTz **1**.

Table 1
Photophysical properties of dyes **6a**–**e** in chloroform (10 μM, air-equilibrated solutions).

Compound	$\lambda_{abs,1P}$ (nm)[a] [ε (M^{-1} cm^{-1})]	$\lambda_{F,1PE}$ (nm)[b]	φ_F[c]	τ_F (ns)[d]	$\lambda_{abs,2P}$ (nm)[f] [σ_{2PA} (GM)][g]	$\lambda_{F,2PE}$ (nm)[h]
6a	529 [4700]	595	0.67	8.9[e]	700 [178], 890 [11]	595
6b	602 [3250]	646	0.39	10.4	700 [491], 900 [12]	640
6c	544 [3100]	616	0.27	5.9	700 [204], 900 [5]	610
6d	532 [12200]	603	0.70	9.1[e]	700 [284], 890 [14]	595
6e	633 [7300]	670	0.19	10.8	710 [1532], 890 [21]	660

[a] Maximum of the LW absorption band in one-photon conditions.
[b] Fluorescence maximum recorded upon one-photon excitation at the LW absorption wavelength.
[c] Fluorescence quantum yield, error *ca.* 15%.
[d] Fluorescence lifetime, error *ca.* 5%.
[e] Average fluorescence lifetime obtained from the two components of the decay: τ_F,1 = 8.6 ns, 66% and τ_F,2 = 9.6 ns, 34%.
[f] Maxima observed in the 2PA spectra.
[g] Corresponding 2PA cross-section values determined by a 2P-excited fluorescence method.
[h] Fluorescence maximum recorded upon two-photon excitation at the maximum of the corresponding 2PA spectra.

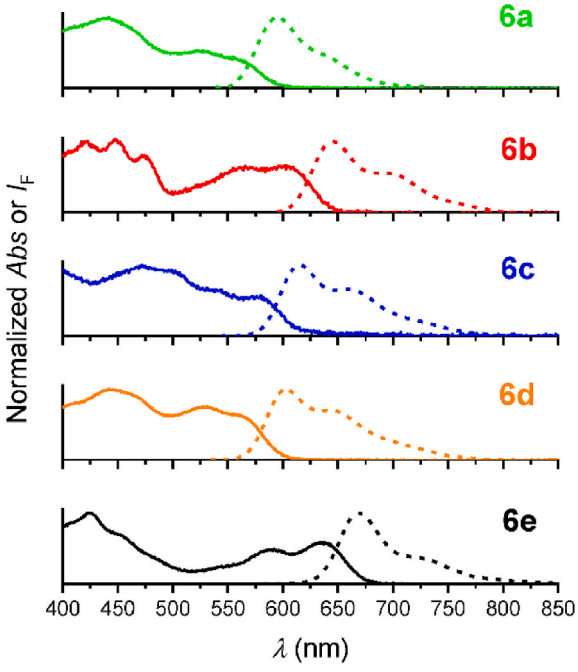

Fig. 2. Normalized absorption (solid lines) and emission (dashed lines) spectra of dyes **6a**–**e** in chloroform (10 μM, air-equilibrated solutions).

absorption energies, although its precision is somewhat reduced for the estimation of emission spectra (see Table 2). However, the experimental-theoretical differences were acceptable in all cases (*i.e.*, differences were below ±0.25 eV) [48,49], and the experimentally observed trends in the emission bands were well reproduced.

Table 2
Calculated electronic and photophysical data for dyes **6a**–**e**.[a]

Compound	Absorption				Emission			
	f[b]	Dominant component (%)[c]	$E_{max,\ calc}$ (eV)[d]	$E_{max,\ exp}$ (eV)[e]	f[b]	Dominant component (%)[c]	$E_{max,\ calc}$ (eV)[d]	$E_{max,\ exp}$ (eV)[e]
6a	0.820	HOMO→LUMO (97)	2.32	2.34	0.784	HOMO←LUMO (98)	1.84	2.08
6b	0.708	HOMO→LUMO (98)	2.14	2.06	0.681	HOMO←LUMO (98)	1.70	1.92
6c	0.752	HOMO→LUMO (97)	2.27	2.28	0.729	HOMO←LUMO (98)	1.80	2.01
6d	0.815	HOMO→LUMO (97)	2.31	2.33	0.774	HOMO←LUMO (98)	1.83	2.06
6e	0.706	HOMO→LUMO (97)	2.02	1.96	0.665	HOMO←LUMO (98)	1.61	1.85

[a] Calculated by means of TD-DFT at the PCM($CHCl_3$)/CAM-B3LYP/6-311+G(2d,p)//PCM($CHCl_3$)/CAM-B3LYP/6-31G(d) level, corresponding to the $S_0 \rightarrow S_1$ (absorption) and $S_0 \leftarrow S_1$ (emission) transitions.
[b] Oscillator strength.
[c] Percentage contribution approximated by $2ci^2 \times 100\%$.
[d] Calculated energies determined in chloroform.
[e] Experimental energies determined in chloroform.

Deepening of the $S_0 \rightarrow S_1$ transition, ascribed to the respective LW absorption band in these dyes, this exclusively involves HOMO and LUMO frontier orbitals, as shown in Fig. 3 (see also Table 2). The HOMO is mainly spread out along the horizontal axis, although some contribution can also be noted in the vertical direction in **6b**–**e**. Nevertheless, this electronic density at the vertical donors was not important in dyes **6c** and **6d**, which contrasts with the observations of **6b** and **6e**. The contribution from the vertical system is especially prominent in the case of **6e**, where both the vertical and horizontal donor groups exhibit similar electron densities and therefore account for the electronic coupling between the two dipolar units. As is common in *push-pull* dyes, the distribution of the electronic density at the LUMO is substantially different from that in the HOMO, with a higher energy molecular orbital placed along the TzQ core.

2.3. Two-photon absorption properties

To ascertain the effectiveness of this novel design concept for the development of 2P-chromophores, the 2PA properties of series **6** in chloroform solution were examined using a 2P-excited fluorescence method [50,51]. In this method, the 2PA cross-section of a chromophore is determined by comparing its 2P-induced fluorescence against a standard compound, whose 2PA cross-section and one-photon fluorescence quantum yield are known (further details are indicated in the Supporting Information) [52,53].

From the 2PA spectra of dyes **6a**–**e** shown in Fig. 4, it can first be concluded that these are considerably more straightforward than the conventional absorption spectra (cf. Fig. 2 and Fig. S1). Moreover, the shape of these spectra was similar for all the derivatives and the most intense 2PA transitions were situated at approximately 700 nm, where σ_{2PA} values above 170 GM were achieved (see Table 1). Notably, the best

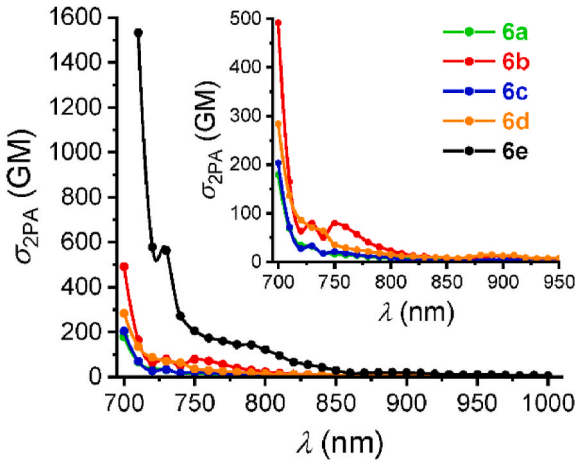

Fig. 4. 2PA spectra of dyes **6a**–**e**. The inset shows a zoom-in for a better visualization of the 2PA spectra of **6a**–**d**.

performing dye was **6e**, yielding an important σ_{2PA} of 1532 GM at 710 nm. As reasoned above for the photophysical properties under 1P conditions, the 2PA properties of these derivatives apparently correlate with the π-conjugation grade attained in the backbones.

Importantly, not only is compound **6e** the stronger 2P-absorber among these analogs, its 2PA properties are also superior to those of our previously reported alkynyl-BTz derivatives. Specifically, the decoration performed over the TzQ core in **6e** results in a 170-fold increase in the σ_{2PA} when comparing this dye with the most similar derivative of our recent work (*i.e.*, alkynyl-BTz with phenyl groups as donor elements in

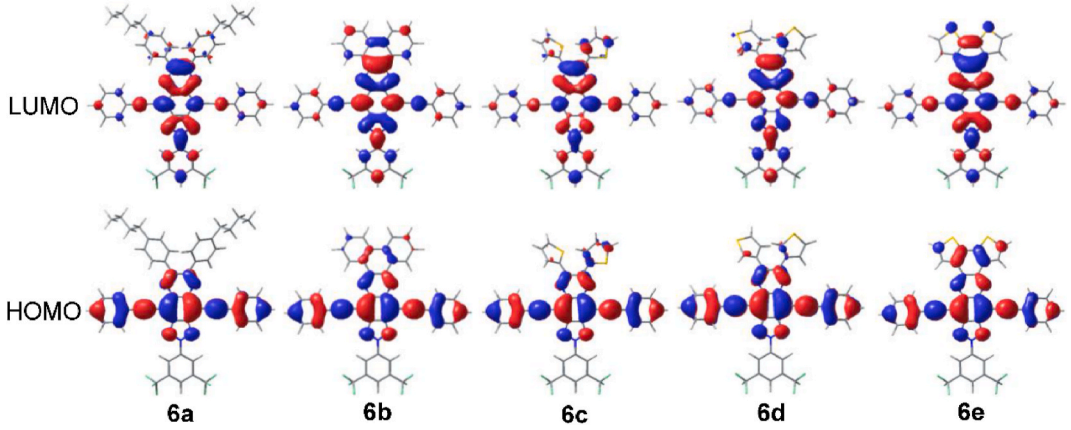

Fig. 3. HOMO and LUMO frontier orbitals associated to the transition $S_0 \rightarrow S_1$ in dyes **6a**–**e** (isosurface: 0.02 e/bohr^3).

the horizontal axis, and without incorporating the TzQ moiety), which demonstrated a discrete σ_{2PA} of 9 GM at 700 nm [28].

In addition, the quadratic dependence of the fluorescence intensity on the laser power applies for all dyes at the corresponding 2P-absorption maxima, thus ensuring the biphotonic nature of the excitation process under the employed experimental conditions (see Fig. S2). The fluorescence spectra obtained under these conditions also resemble those obtained in the conventional regime, as detailed in Table 1 (the 2P-excitation and 2P-excited fluorescence spectra are in Fig. S3); that is, the emissions of these compounds were not dependent on the number of photons involved in the excitation process. Thus, it can be safely assumed the same electronic states are involved in the fluorescence process, regardless of the nature of the excitation process or the attained excited state.

To better understand the optical behavior of these compounds, additional computational calculations were performed. These studies, focused on the 2PA process, do not provide of accurate σ_{2PA} values but offer extremely useful data for elucidating trends in the characteristics of these dyes (see Table S2). These calculations showed that the transition to the first excited state is not allowed under the 2P-regime. Instead, biphotonic excitation results in the attainment of higher electronic excited states. The examination of the calculations reveals two predominant transitions in the 2PA spectra of these compounds, as detailed below.

The analysis of the 1PA and 2PA spectra of **6a** is shown in Fig. 5a; the corresponding analysis on the other dyes are detailed in Figs. S4–S7.

From the previously performed calculations of the absorption energies in 1P-conditions, the $S_0 \rightarrow S_1$ transition can be recognized as the band marked in blue for dye **6a**. According to the 2P-calculations, the first calculated 2P-active transition relates to $S_0 \rightarrow S_2$ (highlighted in purple), and this is active under both excitation conditions. The oscillator strength determined for this transition is higher than that calculated for $S_0 \rightarrow S_1$, which is manifested experimentally through a more intense $S_0 \rightarrow S_2$ band in the conventional absorption (Table 2). In general, calculations also show that this transition is not the most notable in 2P-conditions, which is supported by the experimental σ_{2PA} values determined for the different compounds at the corresponding wavelengths (see Table 1). These observations can be extended to almost all the series, except with **6e**. In this particular case, the same principles apply but over the $S_0 \rightarrow S_3$ transition, which is the first 2P-active transition in this dye (see Fig. S7).

With regard to **6a**, the Natural Transition Orbitals (NTOs), which are a proportional combination of the different elementary orbitals that participate in an electronic event [54], are described in Fig. 5b for $S_0 \rightarrow S_2$ transition. As both NTOs are placed in the vertical axis, this transition appears to be uniquely correlated with the D-A system of the dye. Furthermore, the electronic density over the donor groups in the NTO Hole is displaced to the center of the molecule in the NTO electron, resulting in an almost cyanine-like behavior.

The second 2P-active transition in the theoretical approach is linked to higher excited states. This transition relates to the fourth excited state in **6a**, **c**, and **d**, and is associated to the fifth excited state for **6b** and **6e**. It should be noted that this transition is at roughly twice the energy of the $S_0 \rightarrow S_1$ transition in all the cases, which implies a small detuning energy, *i.e.*, the energy difference between the first excited state and the virtual one is slight. This fact would translate into favoring the overall 2P-driven transition as observed in other type of dyes such as squaraines [55,56], and would explain partially the high cross-section values determined for this higher lying transition. However, and as reasoned below, its interpretation is far more entangled. When considering the NTO hole of these transitions (see Fig. 5b, corresponding to **6a**; see Figs. S4–S7 for other dyes), it is generally observed that this is distributed over the phenyl donor groups and the bis(trifluoromethyl)phenyl moiety. Thus, this transition appears to be associated with the D-π-A-π-D system on the horizontal axis. Nevertheless, the exhaustive analysis of the molecular orbitals that comprise the transition in the different dyes revealed interesting contributions from the vertical dipolar system (see Figs. S8–S12). Remarkably, higher experimental σ_{2PA} values were reached as long as these contributions were significant, that is, the influence of the vertical dipolar system on this transition appeared to underpin the 2PA properties of these dyes. This second 2PA transition was also predicted to be more intense than in previous analyses, which was confirmed by the experimental data.

3. Conclusions

We have proposed an innovative concept for devising improved 2P-chromophores. The orthogonal combination of two dipolar systems within a unique alkynyl-TzQ dye (D-A and D-π-A-π-D at the vertical and horizontal axes, respectively), synthesized through a Stille C–C cross coupling reaction using microwave irradiation as energy source, results in the enhancement of the overall optical properties. This design also incorporates new synthetically tunable positions, which translates into higher versatility. The presence of an improved electron-acceptor core yielded important bathochromic shifts in the both absorption and emission bands relative to our previously reported derivatives. Dyes **6b** and **6e** are especially interesting, with emissions in the red region of the spectrum (almost in the near-infrared), and suggest the potential application of this type of dyes in fields such as bioimaging. Moreover, this strategy has resulted in a remarkable improvement of the 2PA

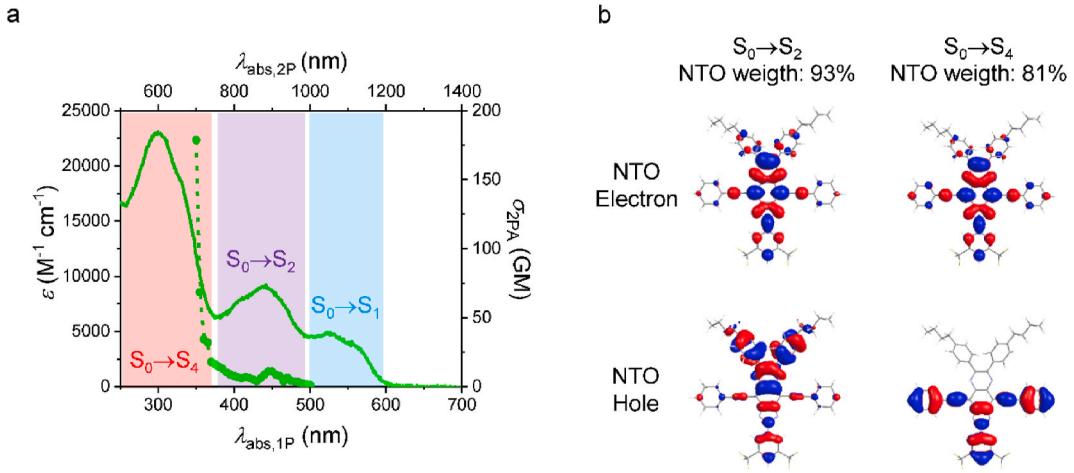

Fig. 5. (a) Comparison between 1PA and 2PA spectra of **6a**, and assignment of the main electronic transitions. (b) NTOs for transitions from the ground state to the second and the fourth excited states in **6a**. The contributions of the NTOs to the respective transitions are indicated for each case (isosurface: 0.02 e/bohr^3).

properties of the dyes. Our best performing dye, **6e**, demonstrated superior 2PA properties that were associated with major electronic communication between the two dipolar systems. This design strategy, which can be readily adapted to other type of scaffolds, may open new avenues for devising new chromophores with powerful 2PA properties.

Author Contributions

Carlos Benitez-Martin: Investigation; Discussion; Original draft preparation; Reviewing and Editing.

Beatriz Donoso: Investigation; Discussion; Original draft preparation.

Iván Torres-Moya: Investigation; Discussion; Original draft preparation.

Jesús Herrera: Investigation; Discussion; Original draft preparation.

Ángel Díaz-Ortiz: Funding acquisition; Supervision; Reviewing and Editing.

Francisco Najera: Funding acquisition; Supervision; Reviewing and Editing.

Pilar Prieto: Funding acquisition; Supervision; Reviewing and Editing.

Ezequiel Perez-Inestrosa: Funding acquisition; Supervision; Reviewing and Editing.

Declaration of competing interest

The authors declare that they have no known competing financial interests or personal relationships that could have appeared to influence the work reported in this paper.

Acknowledgements

E.P.-I. and F.N. acknowledge the Spanish Ministry for Science, Innovation, and Universities (PCI2019-111825-2, and PID2019-104293GB-I00), the Institute of Health Carlos III (ISCIII) RETIC ARADYAL (RD16/0006/0012), the Junta de Andalucıa (UMA18-FEDERJA-007), P. P. acknowledge the supporting of the following project: Project PID2020-119636GB-I00 funded by MCIN/ AEI /10.13039/501100011033 RED2018-102331-T funded by MCIN and Project CTQ2017-84825-R funded by MCIN/ AEI /10.13039/501100011033/ and by FEDER Una manera de hacer Europa and Junta de Comunidades de Castilla-La Mancha (JCCM-FEDER) (Project No. SBPLY/17/180501/000189). C.B.-M. is grateful for a FPU predoctoral contract (FPU16/02516). B. D is grateful for a FPU predoctoral contract (FPU16/05099). I. Torres-Moya thanks to the Junta de Comunidades de Castilla-La Mancha for a post-doctoral contract (SBPLY/19/180501/000346). J. H. is grateful for a predoctoral Junta de Comunidades de Castilla-La Mancha contract (SBPLY/16/180501/000086). The authors would like to thank Pablo Fernández for his assistance in the purification of the products and the work lab. We gratefully acknowledge the ICTS ‘‘NANBIOSIS’’ facilities, more specifically the U28 Unit of the Andalusian Centre for Nanomedicine & Biotechnology (BIONAND) where the 2 PA characterization have been carried out. Finally, we acknowledge the computer resources, technical assistance, and expertise provided by the SCBI (Supercomputing and Bioinformatics) Centre of the University of Málaga and the High Performance Computing Service of UCLM. Funding for open access charge: Universidad de Málaga / CBUA.

Appendix A. Supplementary data

Supplementary data to this article can be found online at https://doi.org/10.1016/j.dyepig.2022.110149.

References

[1] Lim CS, Cho BR. Two-photon probes for biomedical imaging. Tetrahedron 2015;71:8219–49. https://doi.org/10.1016/j.tet.2015.06.083.

[2] Benitez-Martin C, Guadix JA, Pearson JR, Najera F, Perez-Pomares JM, Perez-Inestrosa E. A turn-on two-photon fluorescent probe for detecting lysosomal hydroxyl radicals in living cells. Sensor Actuator B Chem 2019;284:744–50. S0925400518322676.

[3] Benitez-Martin C, Guadix JA, Pearson JR, Najera F, Perez-Pomares JM, Perez-Inestrosa E. Indolenine-based derivatives as customizable two-photon fluorescent probes for pH bioimaging in living cells. ACS Sens 2020;5:1068–74. https://doi.org/10.1021/acssensors.9b02590.

[4] Strickler JH, Webb WW. Two-photon excitation in laser scanning fluorescence microscopy. In: Antos RL, Krisiloff AJ, editors. CAN-AM East. '90, vol. 1398. SPIE; 1991. p. 107–18. https://doi.org/10.1117/12.47787.

[5] Wu E-S, Strickler JH, Harrell WR, Webb WW. In: Cuthbert JD, editor. Two-photon lithography for microelectronic application, vol. 1674. Opt. Microlithogr. V; 1992. p. 776. https://doi.org/10.1117/12.130367. SPIE.

[6] Cumpston BH, Ehrlich JE, Erskine LL, Heikal AA, Hu ZY, Lee IYS, et al. New photopolymers based on two-photon absorbing chromophores and application to three-dimensional microfabrication and optical storage. Mater Res Soc Symp - Proc 1997;488:217–25. https://doi.org/10.1557/proc-488-217. MRS.

[7] Cumpston BH, Ananthavel SP, Barlow S, Dyer DL, Ehrlich JE, Erskine LL, et al. Two-photon polymerization initiators for three-dimensional optical data storage and microfabrication. Nature 1999;398:51–4. https://doi.org/10.1038/17989.

[8] Parthenopoulos DA, Rentzepis PM. Three-dimensional optical storage memory. Science (80-) 1989;245:843–5. https://doi.org/10.1126/science.245.4920.843.

[9] Kawata S, Kawata Y. Three-dimensional optical data storage using photochromic materials. Chem Rev 2000;100:1777–88. https://doi.org/10.1021/cr980073p.

[10] Zhou W, Kuebler SM, Braun KL, Yu T, Cammack JK, Ober CK, et al. An efficient two-photon-generated photoacid applied to positive-tone 3D microfabrication. Science (80-) 2002;296:1106–9. https://doi.org/10.1126/science.296.5570.1106.

[11] Kuebler SM, Braun KL, Zhou W, Cammack JK, Yu T, Ober CK, et al. Design and application of high sensitivity two-photon initiators for three-dimensional microfabrication. J Photochem Photobiol A Chem 2003;158:163–70. https://doi.org/10.1016/S1010-6030(03)00030-3.

[12] Walker E, Rentzepis PM. Two-photon technology: a new dimension. Nat Photonics 2008;2:406–8. https://doi.org/10.1038/nphoton.2008.121.

[13] He GS, Tan L-S, Zheng Q, Prasad PN. Multiphoton absorbing materials: molecular designs, characterizations, and applications. Chem Rev 2008;108:1245–330. https://doi.org/10.1021/cr050054x.

[14] Benitez-Martin C, Li S, Dominguez-Alfaro A, Najera F, Pérez-Inestrosa E, Pischel U, et al. Toward two-photon absorbing dyes with unusually potentiated nonlinear fluorescence response. J Am Chem Soc 2020;142:14854–8. https://doi.org/10.1021/JACS.0C07377.

[15] Rumi M, Perry JW. Two-photon absorption: an overview of measurements and principles. Adv Opt Photon 2010;2:451. https://doi.org/10.1364/aop.2.000451.

[16] Lakowicz JR. Principles of fluorescence spectroscopy. Boston, MA: Springer; 2006. https://doi.org/10.1007/978-0-387-46312-4.

[17] Porres L, Charlot M, Entwistle CD, Beeby A, Marder TB, Blanchard-Desce M. Novel boron quadrupolar NLO-phores: optimization of TPA/transparency trade-off via molecular engineering. In: Yeates AT, editor. Nonlinear Opt. Transm. Multiphot. Process. Org. III, vol. 5934. SPIE; 2005. 59340F. https://doi.org/10.1117/12.618425.

[18] Nguyen KA, Rogers JE, Slagle JE, Day PN, Kannan R, Tan LS, et al. Effects of conjugation in length and dimension on spectroscopic properties of fluorene-based chromophores from experiment and theory. J Phys Chem A 2006;110:13172–82. https://doi.org/10.1021/jp0642645.

[19] Ramakrishna G, Goodson T. Excited-state deactivation of branched two-photon absorbing chromophores: a femtosecond transient absorption investigation. J Phys Chem A 2007;111:993–1000. https://doi.org/10.1021/jp064004n.

[20] Liang X, Zhang Q. Recent progress on intramolecular charge-transfer compounds as photoelectric active materials. Sci China Mater 2017;60:1093–101. https://doi.org/10.1007/S40843-016-5170-2. 6011 2017.

[21] Xu L, Zhu H, Long G, Zhao J, Li D, Ganguly R, et al. 4-Diphenylamino-phenyl substituted pyrazine: nonlinear optical switching by protonation. J Mater Chem C 2015;3:9191–6. https://doi.org/10.1039/C5TC01657F.

[22] Pawlicki MM, Collins HA, Denning RG, Anderson HL. Two-photon absorption and the design of two-photon dyes. Angew Chem Int Ed Engl 2009;48:3244–66. https://doi.org/10.1002/anie.200805257.

[23] Xu L, Lin W, Huang B, Zhang J, Long X, Zhang W, et al. The design strategies and applications for organic multi-branched two-photon absorption chromophores with novel cores and branches: a recent review. J Mater Chem C 2021;9:1520–36. https://doi.org/10.1039/D0TC05910B.

[24] Kato SI, Matsumoto T, Ishi-I T, Thiemann T, Shigeiwa M, Gorohmaru H, et al. Strongly red-fluorescent novel donor-π-bridge-acceptor-π-bridge-donor (D-π-A-π-D) type 2,1,3-benzothiadiazoles with enhanced two-photon absorption cross-sections. Chem Commun 2004:2342–3. https://doi.org/10.1039/b410016f.

[25] Kato S, Matsumoto T, Shigeiwa M, Gorohmaru H, Maeda S, Ishi-i T, et al. Novel 2,1,3-benzothiadiazole-based red-fluorescent dyes with enhanced two-photon absorption cross-sections. Chem - A Eur J 2006;12:2303–17. https://doi.org/10.1002/chem.200500921.

[26] Wang Y, Huang J, Zhou H, Ma G, Qian S, Zhu XH. Synthesis, optical properties and ultrafast dynamics of a 2,1,3-benzothiadiazole-based red emitter with intense fluorescence and large two-photon absorption cross-section. Dyes Pigments 2012;92:573–9. https://doi.org/10.1016/j.dyepig.2011.06.032.

[27] Yao S, Kim B, Yue X, Colon Gomez MY, Bondar MV, Belfield KD. Synthesis of near-infrared fluorescent two-photon-absorbing fluorenyl benzothiadiazole and benzoselenadiazole derivatives. ACS Omega 2016;1:1149–56. https://doi.org/10.1021/acsomega.6b00289.
[28] Torres-Moya I, Benitez-Martin C, Donoso B, Tardío C, Martín R, Carrillo JR, et al. Extended alkenyl and alkynyl benzotriazoles with enhanced two-photon absorption properties as a promising alternative to benzothiadiazoles. Chem Eur J 2019;25:15572–9. https://doi.org/10.1002/chem.201903493.
[29] Yao S, Kim B, Yue X, Gomez MYC, Bondar MV, Belfield KD. Synthesis of near-infrared fluorescent two-photon-absorbing fluorenyl benzothiadiazole and benzoselenadiazole derivatives. ACS Omega 2016;1:1149–56. https://doi.org/10.1021/ACSOMEGA.6B00289.
[30] Ma H, Zhao C, Meng H, Li R, Mao L, Hu D, et al. Multifunctional organic fluorescent probe with aggregation-induced emission characteristics: ultrafast tumor monitoring, two-photon imaging, and image-guide photodynamic therapy. ACS Appl Mater Interfaces 2021;13:7987–96. https://doi.org/10.1021/ACSAMI.0C21309.
[31] David S, Chang H, Lopes C, Brännlund C, Le Guennic B, Berginc G, et al. Benzothiadiazole-Substituted aza-BODIPY dyes: two-photon absorption enhancement for improved optical limiting performances in the short-wave IR range. Chem Eur J 2021;27. https://doi.org/10.1002/chem.202004899. chem.202004899.
[32] Habeeba AU, Saravanan M, Girisun TCS, Anandan S. Nonlinear optical studies of conjugated organic dyes for optical limiting applications. J Mol Struct 2021;1240:130559. https://doi.org/10.1016/J.MOLSTRUC.2021.130559.
[33] Ishi-i T, Taguri Y, Kato S, Shigeiwa M, Gorohmaru H, Maeda S, et al. Singlet oxygen generation by two-photon excitation of porphyrin derivatives having two-photon-absorbing benzothiadiazole chromophores. J Mater Chem 2007;17:3341–6. https://doi.org/10.1039/B704499B.
[34] Hua B, Zhang C, Zhou W, Shao L, Wang Z, Wang L, et al. Pillar[5]arene-Based solid-state supramolecular polymers with suppressed aggregation-caused quenching effects and two-photon excited emission. J Am Chem Soc 2020;142:16557–61. https://doi.org/10.1021/JACS.0C08751.
[35] Shi Y, Salter PS, Li M, Taylor RA, Elston SJ, Morris SM, et al. Two-photon laser-written photoalignment layers for patterning liquid crystalline conjugated polymer orientation. Adv Funct Mater 2021;31:2007493. https://doi.org/10.1002/ADFM.202007493.
[36] Torres I, Carrillo JR, Díaz-Ortiz A, Martín R, Gómez MV, Stegemann L, et al. Self-assembly of T-shape 2H-benzo[d][1,2,3]-triazoles. Optical waveguide and photophysical properties. RSC Adv 2016;6:36544–53. https://doi.org/10.1039/C6RA02473D.
[37] Torres I, Díaz-Ortiz A, Sánchez L, Orduna J, Blesa MJ, Carrillo JR, et al. Tunable emission in aggregated T-Shaped 2H-Benzo[d][1,2,3]triazoles with waveguide behaviour. Dyes Pigments 2017;142:212–25. https://doi.org/10.1016/J.DYEPIG.2017.02.048.
[38] Dallos T, Hamburger M, Baumgarten M. Thiadiazoloquinoxalines: tuning physical properties through smart synthesis. Org Lett 2011;13:1936–9. https://doi.org/10.1021/ol200250e.
[39] Kato SI, Watanabe K, Tamura M, Ueno M, Nitani M, Ie Y, et al. Tetraalkoxyphenanthrene-fused thiadiazoloquinoxalines: synthesis, electronic, optical, and electrochemical properties, and self-assembly. J Org Chem 2017;82:3132–43. https://doi.org/10.1021/acs.joc.7b00084.
[40] Martín R, Prieto P, Carrillo JR, Rodríguez AM, Cozar A de, Boj PG, et al. Design, synthesis and amplified spontaneous emission of 1,2,5-benzothiadiazole derivatives. J Mater Chem C 2019;7:9996–10007. https://doi.org/10.1039/C9TC03148K.
[41] Martín R, Torres-Moya I, Donoso B, Carrillo JR, González-Domínguez JM, Frontiñan-Rubio J, et al. Slow diffusion co-assembly as an efficient tool to tune colour emission in alkynyl benzoazoles. Dyes Pigments 2020;176:108246. https://doi.org/10.1016/J.DYEPIG.2020.108246.
[42] Torres I, Díaz-Ortiz A, Sánchez L, Orduna J, Blesa MJ, Carrillo JR, et al. Tunable emission in aggregated T-Shaped 2H-Benzo[d][1,2,3]triazoles with waveguide behaviour. Dyes Pigments 2017;142:212–25. https://doi.org/10.1016/j.dyepig.2017.02.048.
[43] Gu PY, Zhang J, Long G, Wang Z, Zhang Q. Solution-processable thiadiazoloquinoxaline-based donor-acceptor small molecules for thin-film transistors. J Mater Chem C 2016;4:3809–14. https://doi.org/10.1039/c5tc03222a.
[44] An C, Puniredd SR, Guo X, Stelzig T, Zhao Y, Pisula W, et al. Benzodithiophene–Thiadiazoloquinoxaline as an acceptor for ambipolar copolymers with deep LUMO level and distinct linkage pattern. Macromolecules 2014;47:979–86. https://doi.org/10.1021/ma401938m.
[45] Dallos T, Hamburger M, Baumgarten M. Thiadiazoloquinoxalines: tuning physical properties through smart synthesis. Org Lett 2011;13:1936–9. https://doi.org/10.1021/ol200250e.
[46] Arroyave FA, Richard CA, Reynolds JR. Efficient synthesis of benzo[1,2- b:6,5- b']dithiophene-4,5-dione (BDTD) and its chemical transformations into precursors for π-conjugated materials. Org Lett 2012;14:6138–41. https://doi.org/10.1021/ol302704v.
[47] Cebrián C, de Cózar A, Prieto P, Díaz-Ortiz A, de la Hoz A, Carrillo J, et al. Microwave-assisted Stille reactions as a powerful tool for building polyheteroaryl systems bearing a (1H)-1,2,4-Triazole moiety. Synlett 2010;2010:55–60. https://doi.org/10.1055/s-0029-1218533.
[48] Jacquemin D, Wathelet V, Perpète EA, Adamo C. Extensive TD-DFT benchmark: singlet-excited states of organic molecules. J Chem Theor Comput 2009;5:2420–35. https://doi.org/10.1021/CT900298E.
[49] Shao Y, Mei Y, Sundholm D, Kaila VRI. Benchmarking the performance of time-dependent density functional theory methods on biochromophores. J Chem Theor Comput 2019;16:587–600. https://doi.org/10.1021/ACS.JCTC.9B00823.
[50] Rumi M, Perry JW. Two-photon absorption: an overview of measurements and principles. Adv Opt Photon 2010;2:451. https://doi.org/10.1364/aop.2.000451.
[51] Terenziani F, Katan C, Badaeva E, Tretiak S, Blanchard-Desce M. Enhanced two-photon absorption of organic chromophores: theoretical and experimental assessments. Adv Mater 2008;20:4641–78. https://doi.org/10.1002/adma.200800402.
[52] Terenziani F, Katan C, Badaeva E, Tretiak S, Blanchara-Desce M. Enhanced two-photon absorption of organic chromophores: theoretical and experimental assessments. Adv Mater 2008;20:4641–78. https://doi.org/10.1002/adma.200800402.
[53] Xu L, Zhang J, Yin L, Long X, Zhang W, Zhang Q. Recent progress in efficient organic two-photon dyes for fluorescence imaging and photodynamic therapy. J Mater Chem C 2020;8:6342–9. https://doi.org/10.1039/d0tc00563k.
[54] Martin RL. Natural transition orbitals. J Chem Phys 2003;118:4775–7. https://doi.org/10.1063/1.1558471.
[55] Chung SJ, Zheng S, Odani T, Beverina L, Fu J, Padilha LA, et al. Extended squaraine dyes with large two-photon absorption cross-sections. J Am Chem Soc 2006;128:14444–5. https://doi.org/10.1021/JA065556M.
[56] Chang HJ, Bondar MV, Liu T, Liu X, Singh S, Belfield KD, et al. Electronic nature of neutral and charged two-photon absorbing squaraines for fluorescence bioimaging application. ACS Omega 2019;4:14669–79. https://doi.org/10.1021/ACSOMEGA.9B00718.